

Article

# The Effects of Process Parameters on Workpiece Roundness in the Shoe-Type Centerless Grinding Operation for Internal Raceway of Ball Bearings

Nguyen Anh Tuan 

Faculty of Mechanical Engineering, The Research Team on the Optimization of Mechanical Design and Machining, University of Economics—Technology for Industries (UNETI), No. 456, Minh Khai Str., Hai Ba Trung Dist., Hanoi 11622, Vietnam; natuan.ck@uneti.edu.vn; Tel.: +84-9-6494-5889

**Abstract:** One of the most important indices of bearing raceway, roundness, has an important influence on the life and performance of the bearing. Currently, shoe-type centerless grinding (STCG) is a core process for the fabrication of the raceway surface. Some researchers have carried out studies in this field; however, the reason and extent of the influence of process parameters on the workpiece roundness in the STCG operation for the internal raceway of the 6208 ball bearings are not clear up to now. In this paper, new research on the effects of process parameters on workpiece roundness in the STCG operation for the internal raceway of the 6208 ball bearings is presented. The influence of the angular placement of the two shoes, as well as the technology parameters including the offset between the rotational centers of the workpiece and the magnetic drivehead ( $e$ ), the normal feed rate ( $S_{nf}$ ), the speed of the workpiece ( $n_w$ ), and the grinding depth ( $a_f$ ), on the roundness of the raceway surface were investigated both theoretically and experimentally to solve the difficulties in the STCG operation to ensure the roundness of the raceway surface. Based on the research results, a guideline for selecting initial process parameters is introduced to ensure the roundness of the bearing raceway in the STCG operation for the internal raceway of 6208\_ball bearings on the 3MK136B grinder.

**Keywords:** the shoe-type centerless grinding; the roundness of the bearing raceway; process parameters



**Citation:** Tuan, N.A. The Effects of Process Parameters on Workpiece Roundness in the Shoe-Type Centerless Grinding Operation for Internal Raceway of Ball Bearings. *Coatings* **2023**, *13*, 1864. <https://doi.org/10.3390/coatings13111864>

Academic Editors: Alexander S. Leshin and Vladimir Kashkarov

Received: 3 September 2023

Revised: 22 October 2023

Accepted: 24 October 2023

Published: 31 October 2023



**Copyright:** © 2023 by the author. Licensee MDPI, Basel, Switzerland. This article is an open access article distributed under the terms and conditions of the Creative Commons Attribution (CC BY) license (<https://creativecommons.org/licenses/by/4.0/>).

## 1. Introduction

Bearings are an important product used in almost every type of rotating machinery [1–5]. The manufacturing quality of ball bearings directly affects the performance, quality and reliability of mechanical devices [3–5]. With the development of high-speed, high-precision machinery, etc., the working quality and stability of the bearings are increasingly required [4,5]. For bearing manufacturers, it is particularly important to constantly improve their processing technology to meet market requirements. Thus, numerous studies in the field of bearing manufacturing have been conducted [1–6].

Production of bearings includes many stages of the technological process, in which the manufacturing stage of the raceway surface is one of the most important processing stages [5]. The raceway surface is a critical surface that is difficult to machine but requires high accuracy [1–6]. This is a machined surface with a circular cross-section. The quality of machining the raceway surface directly affects the performance and fatigue life of the bearing, and thus, a strict standard has to be satisfied in the manufacturing processes [3–6].

Grinding is a core process for the fabrication of the raceway surface. There are two types of grinding processes that produce circular cross sections. The process based on the first definition of a circle, establishing a center and a radius, is called “center-type grinding”. Difficulties with this method include the accurate placement of the centers on the workpiece axis, the constant distance maintenance of the grinding wheel during processing, and the deflection of the workpiece due to the bending moment from the cones and the grinding wheel. The second definition of an ideal circle, three points on the circumference, is met

with a process called “centerless grinding”. Centerless grinding optimally constrains the circular workpiece geometry, has high production rates, and can maintain high roundness accuracy [7–9]. Thus, centerless grinding is widely used in industry for the precision machining of cylindrical components [8,9]. However, in conventional centerless grinding, the final accuracy (i.e., roundness) of the workpiece greatly depends on the roundness and the rotational accuracy of the regulating wheel since the workpiece is essentially held along its periphery [10–12]. One of the best ways to solve this problem would be to adopt the shoe-type centerless grinding method, in which a regulating wheel is not required. This processing method makes it possible to ensure high accuracy of the size and shape of products and also a high degree of automation of both machine tools and automatic lines [5,13–16]. Thus, shoe-type centerless grinding (STCG) is a very important method for machining bearing raceways.

However, this grinding process is much more complicated than other grinding methods. The difference between shoe centerless grinding and conventional grinding methods is that the workpiece’s instantaneous center will shift [5,14]. In addition, this grinding process consists of three stages with different parameters (rough grinding stage, fine grinding stage, and spark-out grinding stage). During the grinding process, there are three contact points on the surface of the workpiece. Specifically, the first is the point of contact between the grinding wheel and the workpiece; the second is the support point in the front shoe; and the third is the support point in the rear shoe [15]. The circular geometry of the workpiece in the shoe-type centerless grinding process is determined by three points because of the workpiece contacting the two shoes and the grinding wheel [13]. Therefore, the roundness of the workpiece is greatly influenced by process parameters such as the mounting angle of the support shoes, grinding mode and many other factors [13–16]. Thus, the roundness of the bearing raceway is the key index for evaluating the grinding quality of a bearing raceway.

Many researchers have been involved in the studies of the STCG processes [2–5,13–16]. In 1992, Charmley [16] proposed a model of shoe-type centerless grinding to analyze the effects of the shoe setup angles on the geometric and dynamic stability of the process. Based on that, Charmley predicted final workpiece roundness trends. In 1999, Gan et al. [13] studied the workholding stability in shoe-type centerless grinding process. He concluded that workholding stability is achievable if the driving capability and the constraint capability of the grinding system are balanced [13]. In 2003, Zhang et al. [14] developed a geometry model to predict the lobbing generation and the profile of the workpiece in shoe centerless grinding. Based on the model, important parameters and their relationships are studied [14]. Then, in 2004, H. Zhang et al. [15] also developed a one-degree-of-freedom dynamic model to predict the stability limits of the shoe centerless grinding process and study the crucial parameters, the workpiece shoe set-up and their relationship. Based on the simulation and experiment, it was observed that the set-up angle of the shoe supports is critical to guaranteeing stability. In 2017, Jiang et al. [2] developed the transformation method between the grinding parameters of the plane surface and the raceway surface to predict the value of grinding force, temperature, roughness and dark layer thickness in the inner ring raceway grinding operation. In the same year, Chang et al. [3] studied the effect of wheel speed, workpiece speed and grinding depth on the surface integrity of a bearing raceway in a shoe-type centerless grinding process. Then, the grinding process parameters were optimized by using support vector machine (SVM) models. In 2019, Chang et al. [4] optimized the technological parameters in the process of grinding the bearing surface to minimize the grinding time and maximize material removal rate by using the genetic algorithm NSGA-II. Recently, multi-objective optimization of the process parameters was studied to minimize grindstone wear, maximize material removal rate and the total number of ground parts in a grinding cycle in the shoe-type centerless grinding operation for the inner ring raceway of the ball bearing [5].

However, the effects of process parameters on workpiece roundness in the STCG operation for the internal raceway of ball bearings have not been studied in this research.

In fact, one of the most important technical requirements in this grinding process is the final roundness and accuracy of the machined surface. Thus, this study attempts to solve the difficulties in the STCG operation to ensure the roundness of the raceway surface. The influence of the angular placement of the two shoes, as well as the technology parameters on the roundness of the workpiece was analyzed.

**2. Theoretical Analyses**

*2.1. The Influence of the Workpiece Shoe Setup on the Roundness of the Bearing Raceway in the STCG Process for the Internal Raceway of Ball Bearings*

In the STCG process, the raceway surface of ball bearings is machined. The schematic diagram of this grinding process is shown in Figure 1, where the workpiece is positioned on two fixed shoes with shoe setup angles of  $\beta$  and  $\gamma$ . A magnetic drivehead is used to drive the workpiece in an independent direction, and the displacement between the rotational centers of the workpiece and the magnetic drivehead is intended to force contact between the raceway surface of the ball bearings and two fixed shoes [13]. The contact points between the workpiece and the shoes determine the position of the workpiece in the grinding process.

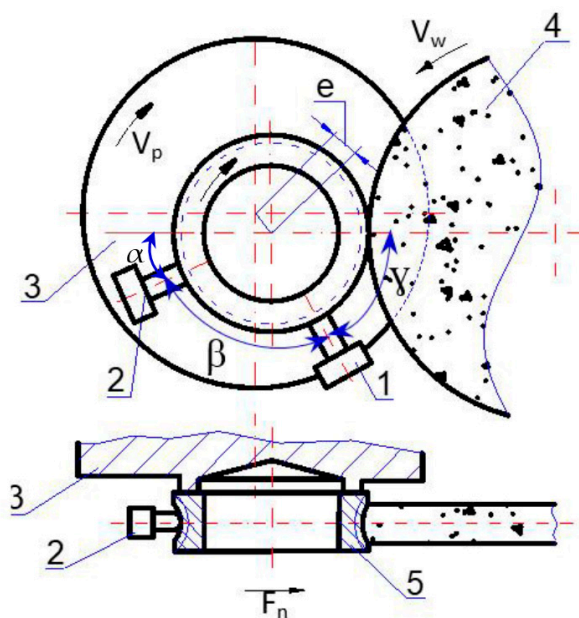


**Figure 1.** The schematic diagram of the STCG process for bearings inner ring raceway [5]. 1: front shoe; 2: rear shoe; 3: magnetic drivehead; 4: grinding wheel; 5: grinding work-piece.

The nominal cross-section of the workpiece is a circle taken as the base circle. Shape deviation in cross-section is usually described by a trigonometric polynomial, since most of the factors in the part profile forming process are cyclical in nature. Therefore, the shape of the raceway surface in the cross-section, generated in the STCG process, will be expressed as a trigonometric polynomial as follows [14]:

$$r = r_0 + \sum_{n=2}^p a_n \sin(n\varphi + \alpha_n) \tag{1}$$

where  $r_0$ : mean radius of the raceway surface in the cross-section;  $n$ : distortion frequency;  $a_n$ : initial amplitude of the  $n$ th harmonics;  $\varphi$ : the rotation angle of workpiece (Polar angle);  $\alpha_n$ : initial phase deviation angle of the  $n$ th harmonics;  $p$ : maximum number of distortion edges of the harmonics.

In the STCG process, the workpiece will continuously rotate. As a result, the cross-sectional center of the workpiece ( $O_1$ ) is always moving. This movement depends on the

roundness of the workpiece and the reduction in the diameter of the workpiece during grinding (as shown in Figure 2). Therefore, the distance between the actual contour center of the workpiece ( $O_1$ ) and the ideal perfectly circular profile center of the workpiece ( $O$ ) in the grinding process is a variable value. After one rotation, the actual contour center of the workpiece will describe a closed contour, representing the base error. In essence, the base error is the deviation of the workpiece in the actual position at the initial preparation ( $O_1$ ) from the required position ( $O$ ). Where the required position of the workpiece ( $O$ ) is the expected position for the workpiece, whose cross-sectional shape is an absolute circle determined by the positions of two fixed shoes on the machine.

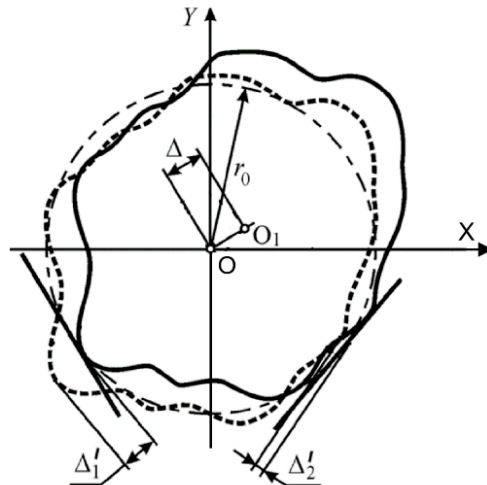


**Figure 2.** The cross-section of the workpiece in the STCG process for bearings inner ring raceway.

Because the workpiece often has roundness and the diameter of the workpiece changes with the grinding time, the instantaneous center of the workpiece ( $O_1$ ) will not be fixed but have a changing position during the STCG process. The amount of instantaneous center displacement of the workpiece ( $\Delta x$ ) together with the amount of change in the radius of the workpiece ( $\Delta r_1$ ) in the  $O_1X$  direction determines the total amount of change in the radius of the workpiece at the point where the workpiece contacts the grinding wheel ( $\Delta x^*$ ) while the instantaneous center of the workpiece ( $O_1$ ) is determined by the radius  $r_2$  and  $r_3$ , corresponding to the radius of the workpiece at the position where the workpiece is in contact with the shoes at points K and L (as shown in Figure 3). Thus, the formula for determining  $\Delta x^*$  is as follows:

$$\Delta x^* = \Delta r_1 + \Delta x \quad (2)$$

where  $\Delta x$ : the amount of instantaneous center displacement of the workpiece in the  $O_1X$  direction;  $\Delta r_1$ : the value of the radius change of the workpiece in the  $O_1X$  direction. It is also the value of radius change of the workpiece at position P;  $\Delta x^*$ : the total amount of change in the radius of the workpiece at the point where the workpiece contacts the grinding wheel.

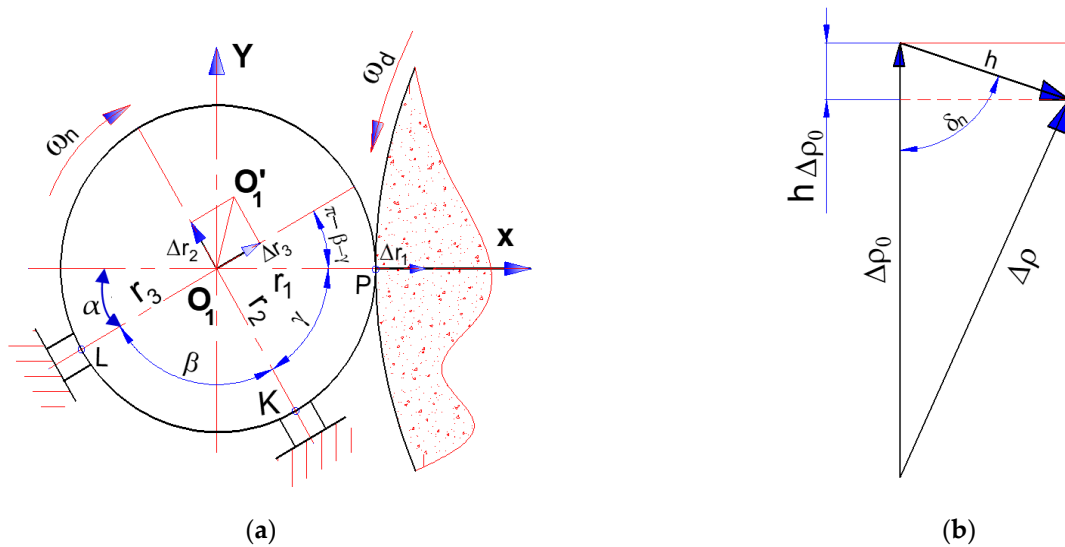


**Figure 3.** The diagram of geometric relationship for a typical setup in the STCG process. (a) A typical setup of the shoe-type centerless grinding process; (b) the shape deviation change of the workpiece in the shoe-type centerless.

While:

$$\Delta x = \frac{\Delta r_3 \sin \gamma - \Delta r_2 \sin(\beta + \gamma)}{\sin \beta} \tag{3}$$

where:  $\beta, \gamma$ : the values of shoe angle (as shown in Figure 3);  $\Delta r_2$ : the value of the radius change of the workpiece at position K;  $\Delta r_3$ : the value of the radius change of the workpiece at position L.

Since then:

$$\Delta x^* = \Delta r_1 + \frac{\Delta r_3 \sin \gamma - \Delta r_2 \sin(\beta + \gamma)}{\sin \beta} \tag{4}$$

On the other hand, the radius change of the workpiece is a function of the rotation angle of the workpiece ( $\varphi$ ) and can be described by the Fourier polynomial as follows:

$$\Delta r_\varphi = a_1 \sin(\varphi + \alpha_1) + a_2 \sin(2\varphi + \alpha_2) + \dots + a_n \sin(n\varphi + \alpha_n) + \dots \tag{5}$$

where:  $a_n$ : the amplitude of the  $n$ th harmonics;  $\alpha_n$ : initial phase deviation angle of the  $n$ th harmonics;  $\varphi$ : the rotation angle of workpiece;  $\Delta r_\varphi$ : the value of the radius change of the workpiece.

In Figure 3  $\Delta \rho_0$ : the initial shape deviation of the workpiece;  $\Delta \rho$ : the current shape deviation of the part;  $h$ : metal removal volume.

Thus, the value of the radius change of the workpiece at 3 positions P, K, L (as shown in Figure 3) is determined through the mounting angles  $\beta, \gamma$  as follows:

$$\begin{aligned} \Delta r_1 &= \sum_{n=1}^{\infty} a_n \sin(n\varphi + \alpha_n) \\ \Delta r_2 &= \sum_{n=1}^{\infty} a_n \sin[n(\varphi + \gamma) + \alpha_n] \\ \Delta r_3 &= \sum_{n=1}^{\infty} a_n \sin[n(\varphi + \gamma + \beta) + \alpha_n] \end{aligned} \tag{6}$$

where:  $\Delta r_1$ : the value of radius change of the workpiece at position P;  $\Delta r_2$ : the value of the radius change of the workpiece at position K;  $\Delta r_3$ : the value of the radius change of the workpiece at position L.

Therefore, the combination of Equations (4)–(6) will determine the total amount of radius variation of the workpiece at the position of the workpiece in contact with the grinding wheel ( $\Delta x^*$ ) according to the following formula:

$$\Delta x^* = \sum_{n=2}^{\infty} a_n b_n \sin(n\varphi + \alpha_n + \delta_n) \quad (7)$$

where:

$$\begin{aligned} b_n &= \sqrt{C_n^2 + D_n^2} \\ C_n &= 1 - \frac{\sin(\gamma+\beta)}{\sin\beta} \cos n\beta + \frac{\sin\gamma}{\sin\beta} \cos n(\gamma + \beta) \\ D_n &= \frac{\sin\gamma}{\sin\beta} \sin n(\gamma + \beta) - \frac{\sin(\gamma+\beta)}{\sin\beta} \sin n\gamma \\ tg\delta_n &= \frac{D_n}{C_n} \end{aligned} \quad (8)$$

In addition, the metal removal volume ( $h$ ) is proportional to the stiffness of the technological system and the total amount of radius variation of the workpiece at the position of the workpiece in contact with the grinding wheel ( $\Delta x^*$ ). Therefore, the metal removal volume ( $h$ ) in the grinding process is determined as follows:

$$h = j \cdot K_p \cdot \Delta x^* \quad (9)$$

where:  $K_p$ : cutting force factor;  $j$ : characteristic quantity for the rigidity of the technological system.

Therefore:

$$h = j \cdot K_p \cdot a_n \cdot b_n \cdot \sin(n\varphi + \alpha_n + \delta_n) = h_0 \cdot \sin(n\varphi + \alpha_n + \delta_n) \quad (10)$$

where:

$$h_0 = j \cdot K_p \cdot a_n \cdot b_n$$

Thus, the metal removal volume is a harmonic function, whose value decreases after each rotation of the workpiece. Based on that, the amount of reduction in the shape deviation of the part in the cross section (the amount of reduction in the roundness of the part) after each rotation of the workpiece is determined by the following formula:

$$h_{\Delta\rho_0} = h_0 \cdot \cos\delta_n = j \cdot K_p \cdot a_n \cdot b_n \cdot \cos\delta_n \quad (11)$$

With:  $b_n^* = b_n \cdot \cos\delta_n$

Since then:

$$h_{\Delta\rho_0} = j \cdot K_p \cdot a_n \cdot b_n^* \quad (12)$$

It is found that the value  $b_n^*$  will determine the initial error correction strength and is the correction factor for the shape deviation of the part in the cross section.

- If  $b_n^* = 0$ , the deviation of the original shape of the workpiece will not be corrected.
- If  $b_n^* > 0$ , the roundness deviation of the workpiece will be corrected. Then, the smaller the angle  $\delta_n$  (ie, the larger the  $\cos\delta_n$ ) and the larger the value of the coefficient, the more the grinding process will correct the original shape deviation of the workpiece.
- If  $b_n^* < 0$ , the original shape deviation of the workpiece during grinding will increase.
- The value of the coefficient  $b_n^*$  depends on the mounting angles of the two shoes ( $\beta, \gamma$ ) and can be determined by Formula (8).

Based on the above analysis, it is found that the roundness of the bearing raceway in the shoe-type centerless grinding process depends on the movement trajectory of the workpiece center and the stability in the rotation of the workpiece. The movement trajectory of the workpiece center depends on the mounting angle of the two supports and the deviation of the original shape of the workpiece.

## 2.2. The Influence of the Some Technical Parameters on the Roundness of the Bearing Raceway in the STCG Process for the Internal Raceway of Ball Bearings

In the STCG process for the internal raceway of ball bearings, the roundness of the bearing raceway is also affected by the offset between the rotational centers of the workpiece and the magnetic drivehead ( $e$ ), the normal feed rate ( $S_{nf}$ ), the speed of the workpiece ( $n_w$ ), and the grinding depth ( $a_f$ ).

In this grinding scheme, to ensure a stable position of the workpiece during the grinding, the center of the workpiece will be offset from the center of the magnetic drivehead by a distance of  $e$  (as shown in Figure 4). Thus, the relative sliding speed of the workpiece along the magnetic pole surface will be generated in the grinding process to create a push force (which is the friction force  $F$ ) to force the workpiece's raceway surface to be in contact with two fixed shoes. The magnitude of the friction force ( $F$ ) is proportional to the magnitude of the pressure of the workpiece against the magnetic pole surface ( $Q$ ) and the offset ( $e$ ) [13]. The direction of this frictional force is perpendicular to the line connecting the rotational centers of the workpiece and the magnetic drivehead (as shown in Figure 4). When the offset ( $e$ ) increases, the wear of the magnetic pole surface increases due to the increased sliding process. When reducing the offset ( $e$ ), there is a risk of sliding the workpiece out of the two supports, especially for workpieces with large geometrical deviations.

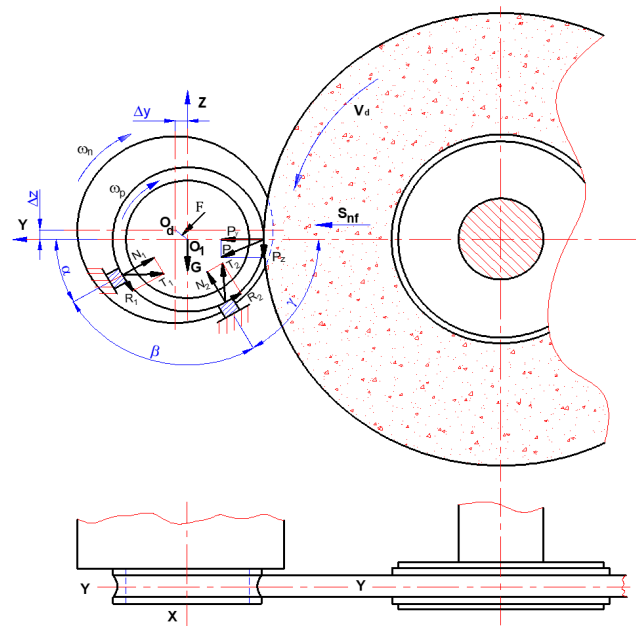


**Figure 4.** The schematic diagram of the forces acting on the workpiece in STCG process for internal raceway of ball bearings [13].

In Figure 4,  $G$ : weight of workpiece;  $P$ : cutting force (which is analyzed into two components of normal force ( $P_y$ ) and tangential force ( $P_z$ );  $N_1$  and  $N_2$ : the reaction force of the shoes on the workpiece;  $R_1$  and  $R_2$ : the friction force between the workpiece and the shoes.

In addition, the motion of feed per revolution in the grinding process is created by the combination of two movements, including the normal feed movement and the rotational motion of the workpiece. If the normal feed rate increases or the rotation speed of the workpiece decreases, the value of cutting depth for one revolution will increase. Therefore, when the rotation feed rate increases or the rotation speed of the workpiece decreases, the uneven distribution of residuals along the circumference of the workpiece surface will increase, leading to an increase in the roundness of the bearing raceway in the shoe-type centerless grinding process.

### 3. Experimental Study and Discussion

#### 3.1. Experimental Setup

Experimental equipment is a 3MK136B bearing raceway grinder with a Chinese grinding wheel marked 500x8x203WA100xLV60 to grind the inner ring groove of a model 6208 ball bearings. The experimental setup is schematically shown in Figure 5. The specifications of the grinding conditions and grinding wheels are shown in Tables 1 and 2.

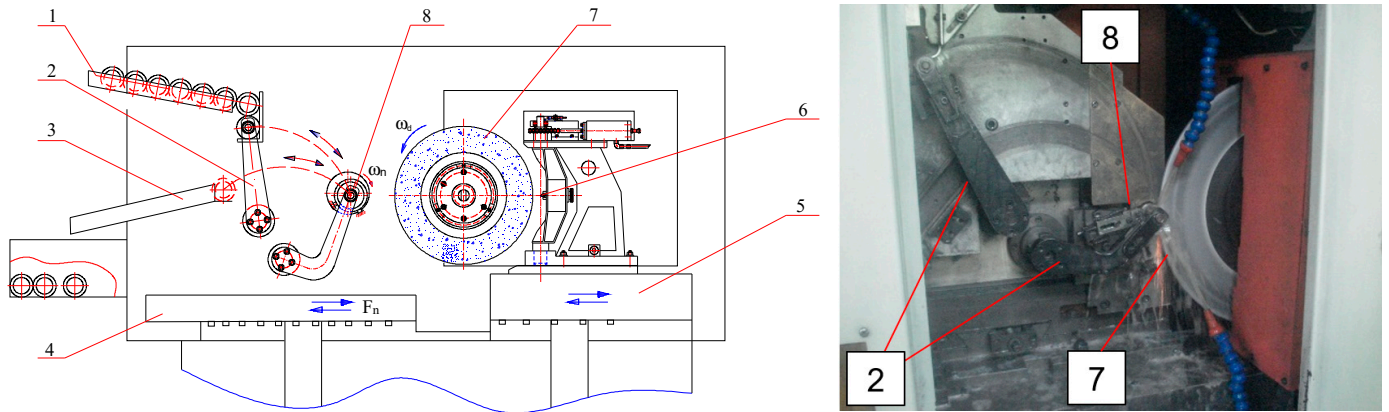
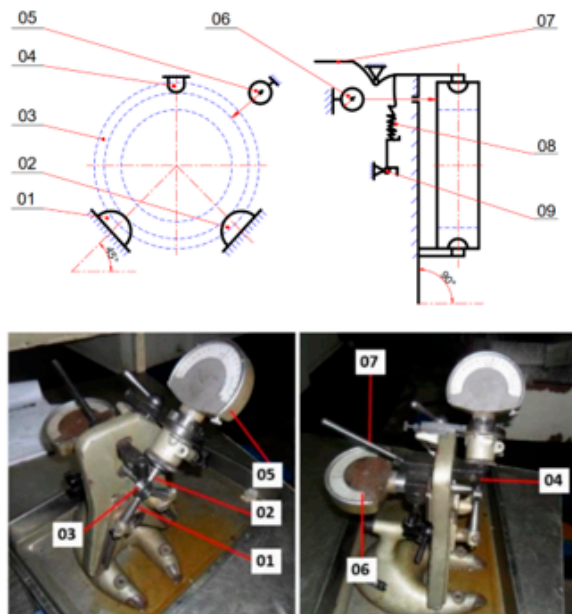


**Figure 5.** The schematic diagram and realistic image of 3MK136B bearing raceway grinder. 1. Charging trough; 2. swing arm of grinder loads/unloads automatically; 3. discharging trough; 4. the workbench; 5. dressing carriage; 6. diamond pen; 7. grinding wheel; 8. workpiece.

The oval of raceway bottom diameter is measured by a D022 measurement equipment made in China as shown in Figure 6.



- 1, 2: Two lock pins.
- 3: The inner ring of ball bearing.
- 4: The pin.
- 5, 6: The measuring meter.
- 7: The lever.
- 8: Springs.
- 9: fixed support.

**Figure 6.** Images and diagram for structural principle of the measurement equipment D022 [5].

**Table 1.** Specifications of grinding conditions.

No	Technical Specifications	Name/Value
1	Grinding machine	3MK136B bearing raceway grinder (made in China)
2	Material of workpiece	SUJ2 alloy steel
3	Hardness	60 ÷ 65 HRC
4	Grinding method	The shoe-type centerless grinding

**Table 2.** Specifications of grinding wheel.

JIS Code	Grade	Grain	Bond	Dimensional Parameters of Grinding Wheel (mm)
3WA100xLV60	Soft	White fused alumina	Vitrified	500 × 8 × 20

### 3.2. Experiment to Determine the Influence of the Workpiece Shoe Setup on the Roundness of the Bearing Raceway in the STCG Process for the Internal Raceway of Ball Bearings

Based on a number of pre-trials at Pho Yen Mechanical Joint Stock Company, the following input parameters were used in this experiment:

- Grinding wheel speed: 60 m/s
- Workpiece speed: 12 m/min
- The normal feed rate of fine grinding: 12.5  $\mu\text{m/s}$
- The normal feed rate of rough grinding: 30  $\mu\text{m/s}$
- The depth of rough grinding: 120  $\mu\text{m}$
- The depth of fine grinding: 15  $\mu\text{m}$
- The offset between the rotational centers of the workpiece and the magnetic drivehead: 0.4 mm.
- The number of ground parts in one cycle: 1 part/1 cycle.
- The values of shoe angle at different levels in this experiment are selected as shown in Table 3.

**Table 3.** Experiment Plans and the Output Response.

No.	The Values of Shoe Angle			The Value of the Coefficient	The 3-Sided Distortion Value of the Workpiece before Processing ( $\mu\text{m}$ )	The 3-Sided Distortion Value of the Part after Processing ( $\mu\text{m}$ )
	$\alpha$	$\beta$	$\gamma$	$b_n^*$		
1	105°	30°	45°	0	20.0	20.0
2	95°	25°	60°	−0.140	20.0	23.0
3	10°	125°	45°	+0.048	20.0	3.5

Based on the experimental results as shown in Table 3, some findings can be presented as follows:

- If the value of the shoe angles is set with  $\alpha = 105^\circ$ ,  $\beta = 30^\circ$ ,  $\gamma = 45^\circ$ , then when substituting these values into Equation (8), we will see the coefficient  $b_n^* = 0$ . In this case, experimental results show that the grinding process cannot correct the roundness deviation of the workpiece. The 3-sided distortion value of the workpiece before machining and after machining does not change.
- If the value of the shoe angles is set with  $\alpha = 95^\circ$ ,  $\beta = 25^\circ$ ,  $\gamma = 60^\circ$ , then when substituting these values into Equation (8), we will see the coefficient  $b_n^* = -0.14$ . In this case, experimental results show that the grinding process cannot correct the roundness of the workpiece. The 3-sided distortion value of the workpiece during grinding will increase. The 3-sided distortion value of the part after grinding will be greater than the 3-sided distortion value of the workpiece before processing.

- If the value of the shoe angles is set with  $\alpha = 10^\circ$ ,  $\beta = 125^\circ$ ,  $\gamma = 45^\circ$ , then when substituting these values into Equation (8), we will see the coefficient  $b_n^* = 0.048$ . In this case, experimental results show that the roundness of the workpiece will be corrected in the grinding process. The 3-sided distortion value of the part after grinding will be much smaller than the 3-sided distortion value of the workpiece before processing.

This proves that the above experimental results are consistent with the theoretical basis established in Section 2.1. Thus, the implementation of the workpiece shoe set-up will impact on the workpiece roundness in the shoe-type centerless grinding process for internal raceway of ball bearings. The mounting angle of the two supports should be adjusted to  $\alpha = 10^\circ$ ,  $\beta = 125^\circ$ ,  $\gamma = 45^\circ$  preferably.

### 3.3. Experiment to Determine the Influence of the Offset between the Rotational Centers of the Workpiece and the Magnetic Drivehead ( $e$ ) on the Workpiece Roundness in the STCG Process for the Internal Raceway of Ball Bearings

Based on a number of pre-trials at Pho Yen Mechanical Joint Stock Company, the following input parameters were used in this experiment:

- Front shoe angle:  $\alpha = 10^\circ$
- Rear shoe angle:  $\beta = 125^\circ$ ,  $\gamma = 45^\circ$
- Grinding wheel speed: 60 m/s
- Workpiece speed: 12 m/min
- The normal feed rate of fine grinding:  $12.5 \mu\text{m/s}$
- The normal feed rate of rough grinding:  $30 \mu\text{m/s}$
- The depth of rough grinding:  $120 \mu\text{m}$
- The depth of fine grinding:  $10 \mu\text{m}$ ;  $20 \mu\text{m}$ ;  $30 \mu\text{m}$ ;  $40 \mu\text{m}$ ;  $50 \mu\text{m}$ ;  $60 \mu\text{m}$ .
- The offset between the rotational centers of the workpiece and the magnetic drivehead:  $0.2 \text{ mm}$ ;  $0.3 \text{ mm}$ ;  $0.4 \text{ mm}$ ;  $0.5 \text{ mm}$ .
- The number of ground parts in one cycle: 1 part/1 cycle.

After carrying out experiments and collecting results, data are analyzed and processed. The ovality and 3-sided distortion value of the raceway bottom surface are determined after each test. Based on the measurement results, using an application of Matlab software, the diagrams showing the influence of grinding depth, the offset between the rotational centers of the workpiece and the magnetic drivehead on the ovality and multi-edge of the part in the shoe-type centerless grinding process for internal raceway of ball bearings, were built as shown in Figure 7.

In Figure 7, the first curve and the second curve are, respectively, the ovality and 3-sided distortion values of the raceway bottom surface according to the depth of fine grinding when the offset between the rotational centers of the workpiece and the magnetic drivehead is  $0.4 \text{ mm}$ . The third curve and the fourth curve of Figure 7 are, respectively, the ovality and 3-sided distortion values of the raceway bottom surface according to the depth of fine grinding when the offset between the rotational centers of the workpiece and the magnetic drivehead is  $0.5 \text{ mm}$ . The fifth curve and the sixth curve of Figure 7 are, respectively, the ovality and 3-sided distortion values of the raceway bottom surface according to the depth of fine grinding when the offset of the workpiece with respect to the drivehead is  $0.3 \text{ mm}$ . The seventh curve and the eighth curve of Figure 7 are, respectively, the ovality and 3-sided distortion values of the raceway bottom surface according to the depth of fine grinding when the offset of the workpiece with respect to the drivehead is  $0.2 \text{ mm}$ .

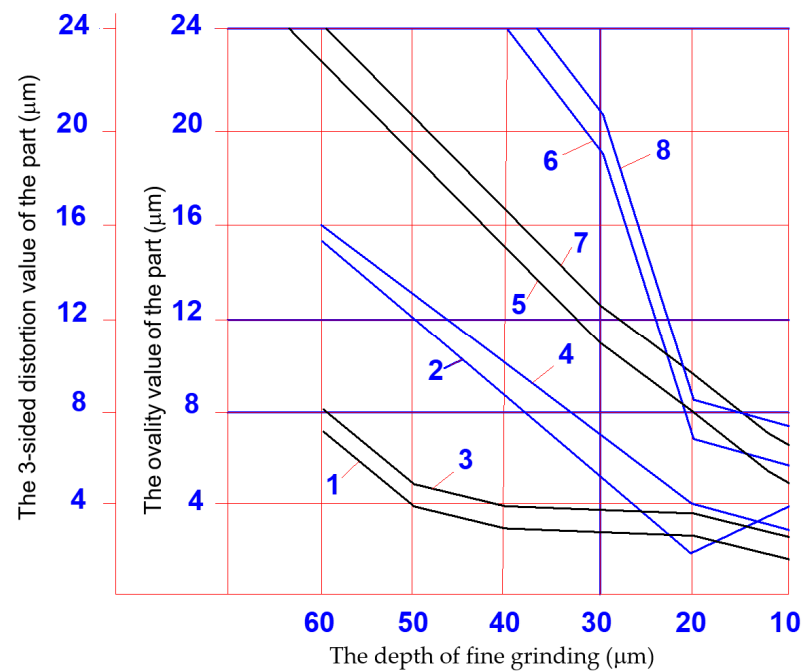


**Figure 7.** The influence of grinding depth on the ovality and multi-edge of the part in the STCG process for internal raceway of ball bearings.

Based on the above graphs, it is found that when the depth of fine grinding increases, the ovality and 3-sided distortion value of the raceway bottom surface will increase. Especially when the offset between the rotational centers of the workpiece and the magnetic drivehead is 0.4 mm, the ovality and 3-sided distortion of the grinding part will be the smallest in experimental cases with different offsets. The reason for this is that the larger the offset, the larger the driving force, but the smaller the driving torque [13]. When the offset increases, the wear of the magnetic pole surface increases. When decreasing the offset, the stability of the workpiece is reduced. Thus, the implementation of the workpiece shoe set-up will affect the offset, leading to an impact on the workpiece roundness in the shoe-type centerless grinding process for the internal raceway of ball bearings. The offset should be adjusted to 0.4 mm, preferably.

#### 3.4. Experiment to Determine the Influence of the Number of Ground Parts on the Workpiece Roundness in the STCG Process for the Internal Raceway of Ball Bearings

Based on the experimental results in the previous section, the following input parameters were used in the second experiment:

- Front shoe angle:  $\alpha = 10^\circ$
- Rear shoe angle:  $\beta = 125^\circ, \gamma = 45^\circ$
- Grinding wheel speed: 60 m/s
- Workpiece speed: 12 m/min
- The normal feed rate of fine grinding:  $12.5 \mu\text{m/s}$
- The normal feed rate of rough grinding:  $30 \mu\text{m/s}$
- The depth of rough grinding:  $120 \mu\text{m}$
- The depth of fine grinding:  $15 \mu\text{m}$
- The offset between the rotational centers of the workpiece and the magnetic drivehead: 0.4 mm.
- The number of ground parts in one cycle: 30 part/1 cycle.

Based on the measurement results, using an application of Matlab software, the diagrams showing the influence of the number of ground parts on the ovality of the part in

the shoe-type centerless grinding process for internal raceway of ball bearings were built as shown in Figure 8.

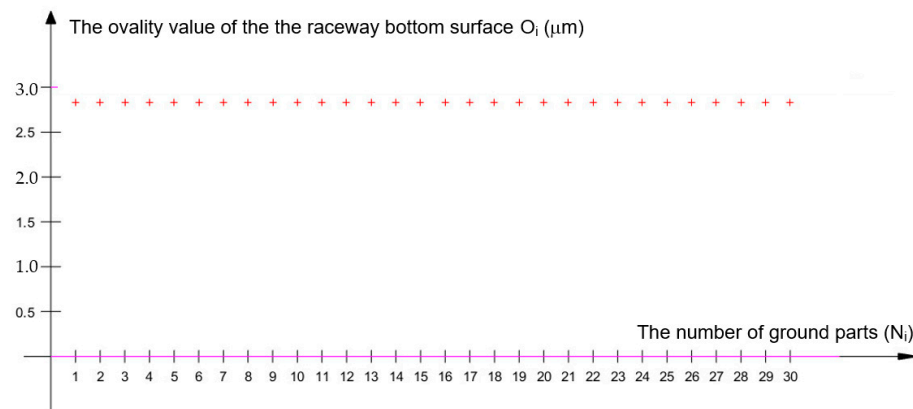


**Figure 8.** The influence of the number of ground parts on the ovality value of the part in the STCG process for internal raceway of ball bearings.

Based on the above diagram, it can be seen that the ovality value of the part does not depend on the number of ground parts in one cycle. The reason is that when the number of parts in a grinding cycle ( $N_i$ ) increases, the grinding time and grinding wheel wear will also increase. However, this does not affect the groove bottom's diameter deviation for grinding parts at different cross sections. Thus, the number of parts in a single cycle ( $N_i$ ) does not affect the part's oval ( $O_i$ ).

### 3.5. Experiment to Determine the Influence of the Technical Parameters on the Workpiece Roundness in the STCG Process for the Internal Raceway of Ball Bearings

Based on the experimental results in the previous sections and a number of pre-trials at Pho Yen Mechanical Joint Stock Company, the values of input parameters at different levels in this experiment are chosen as shown in Table 4. The values of other parameters are the same as those in the third experiment and are kept constant throughout the experiment.

**Table 4.** Input process parameters and design levels.

No.	Input Parameters	Label	Unit	Experimental Levels		
				Low Level	Base Level	High Level
1	The normal feed rate of fine grinding	$S_{nf}$	$\mu\text{m/s}$	5.0	12.5	20.0
2	The speed of the workpiece	$V_w$	m/min	6.0	12.0	18.0
3	The depth of fine grinding	$a_f$	$\mu\text{m}$	10	15	20

With three factors, each factor changes to three levels; thus, it is essential to select the orthogonal experiment matrix  $L_{27}(3^3)$ . In other words, 27 sets of experimental parameters have been implemented (as shown in Table 5). Each set of experimental parameters was conducted three times, and after each experiment, the ovality value of the raceway bottom diameter was measured to determine the average ovality value. The ovality value of the raceway bottom diameter is measured by the D022 measurement equipment made in China (as shown in Figure 6). After carrying out experiments and collecting results, the data are analyzed and processed.

Table 5. Experimental data from 27 experiments.

No.	Input Parameters						The Ovality Value of the Raceway Bottom Diameter								
	Experimental Variables			Encoding Variables			O <sub>1</sub> (μm)	y <sub>1</sub> Ln(O <sub>1</sub> )	O <sub>2</sub> (μm)	y <sub>2</sub> Ln(O <sub>2</sub> )	O <sub>3</sub> (μm)	y <sub>3</sub> Ln(O <sub>3</sub> )	O <sub>mean</sub> (μm)	y <sub>mean</sub> Ln(O <sub>mean</sub> )	
	S <sub>nf</sub> (μm/s)	V <sub>w</sub> (m/min)	a <sub>f</sub> (μm)	x <sub>1</sub> (LnS <sub>nf</sub> )	x <sub>2</sub> (LnV <sub>w</sub> )	x <sub>3</sub> (Lna <sub>f</sub> )									
1	5	6	10	1.6094	1.7918	2.3026	2.5	0.9163	2.5	0.9163	2.5	0.9163	2.5	0.9163	
2	5	12	10	1.6094	2.4849	2.3026	2.0	0.6931	2.0	0.6931	3.0	1.0986	2.3	0.8473	
3	5	18	10	1.6094	2.8904	2.3026	2.0	0.6931	2.0	0.6931	2.5	0.9163	2.2	0.7732	
4	12.5	6	10	2.5257	1.7918	2.3026	3.0	1.0986	3.0	1.0986	3.0	1.0986	3.0	1.0986	
5	12.5	12	10	2.5257	2.4849	2.3026	2.5	0.9163	2.5	0.9163	3.0	1.0986	2.7	0.9808	
6	12.5	18	10	2.5257	2.8904	2.3026	2.5	0.9163	2.5	0.9163	3.0	1.0986	2.7	0.9808	
7	20	6	10	2.9957	1.7918	2.3026	3.5	1.2528	3.5	1.2528	4.0	1.3863	3.7	1.2993	
8	20	12	10	2.9957	2.4849	2.3026	3.0	1.0986	3.5	1.2528	3.5	1.2528	3.3	1.2040	
9	20	18	10	2.9957	2.8904	2.3026	3.0	1.0986	3.0	1.0986	3.5	1.2528	3.2	1.1527	
10	5	6	15	1.6094	1.7918	2.7081	2.5	0.9163	3.0	1.0986	3.0	1.0986	2.8	1.0415	
11	5	12	15	1.6094	2.4849	2.7081	2.5	0.9163	2.5	0.9163	3.0	1.0986	2.7	0.9808	
12	5	18	15	1.6094	2.8904	2.7081	2.5	0.9163	2.5	0.9163	2.5	0.9163	2.5	0.9163	
13	12.5	6	15	2.5257	1.7918	2.7081	3.0	1.0986	3.0	1.0986	3.5	1.2528	3.2	1.1527	
14	12.5	12	15	2.5257	2.4849	2.7081	2.5	0.9163	3.0	1.0986	3.0	1.0986	2.8	1.0415	
15	12.5	18	15	2.5257	2.8904	2.7081	2.5	0.9163	3.0	1.0986	3.0	1.0986	2.8	1.0986	
16	20	6	15	2.9957	1.7918	2.7081	3.5	1.2528	4.0	1.3863	4.0	1.3863	3.8	1.3437	
17	20	12	15	2.9957	2.4849	2.7081	3.5	1.2528	3.5	1.2528	3.5	1.2528	3.5	1.2528	
18	20	18	15	2.9957	2.8904	2.7081	3.0	1.0986	3.5	1.2528	3.5	1.2528	3.3	1.2040	
19	5	6	20	1.6094	1.7918	2.9957	3.0	1.0986	3.5	1.2528	3.5	1.2528	3.3	1.2040	
20	5	12	20	1.6094	2.4849	2.9957	2.5	0.9163	3.0	1.0986	3.0	1.0986	2.8	1.0415	
21	5	18	20	1.6094	2.8904	2.9957	2.5	0.9163	2.5	0.9163	3.0	1.0986	2.7	0.9808	
22	12.5	6	20	2.5257	1.7918	2.9957	3.0	1.0986	3.0	1.0986	3.5	1.2528	3.2	1.1527	
23	12.5	12	20	2.5257	2.4849	2.9957	3.0	1.0986	3.0	1.0986	3.0	1.0986	3.0	1.0986	
24	12.5	18	20	2.5257	2.8904	2.9957	3.0	1.0986	3.0	1.0986	3.0	1.0986	3.0	1.0986	
25	20	6	20	2.9957	1.7918	2.9957	3.5	1.2528	4.0	1.3863	4.0	1.3863	3.8	1.3437	
26	20	12	20	2.9957	2.4849	2.9957	3.5	1.2528	3.5	1.2528	4.0	1.3863	3.7	1.2993	
27	20	18	20	2.9957	2.8904	2.9957	3.5	1.2528	3.5	1.2528	3.5	1.2528	3.5	1.2528	

Based on the above analysis results as well as mathematical models of previous studies [4], the part’s oval (O<sub>i</sub>) can be hypothesized as products of exponents of the input variables (S<sub>nf</sub>, V<sub>w</sub>, a<sub>f</sub>).

$$O_i = c_{01} \cdot S_{nf}^{c_1} \cdot V_w^{c_2} \cdot a_f^{c_3} \tag{13}$$

Linearizing the above nonlinear equation by the logarithm of both sides of the above equations, we obtained:

$$\ln(O_i) = \ln(c_{01}) + c_1 \ln(S_{nf}) + c_2 \ln(V_w) + c_3 \ln(a_f) \tag{14}$$

Define:

$$y_1 = \ln(O_i); c_0 = \ln(c_{01});$$

$$x_1 = \ln(S_{nf}); x_2 = \ln(V_w); x_3 = \ln(a_f);$$

Thus:

$$y_1 = c_0 + c_1 \times 1 + c_2 \times 2 + c_3 \times 3 \tag{15}$$

Therefore, the first-order model was used to represent the mathematical relationship between input parameters and output responses in this study. The coefficients of this model ( $c_0, c_1, c_2, c_3$ ) were defined by applying the regression approach with the least-squares method. Equation (14) can be written in matrix form as follows:

$$[Y_1] = [X].[C] \quad (16)$$

$$[X]^T.[Y_1] = [X]^T.[X].[C] \quad (17)$$

Define:

$$[M] = [X]^T.[X] \quad (18)$$

Thus:

$$[C] = [M]^{-1} . [X]^T.[Y_1] \quad (19)$$

Based on 27 sets of experimental results (as shown in Table 5), the Matlab software version 2021 application can determine  $[M], [M]^{-1}, [C]$  of Equation (19) as follows:

$$[M] = \begin{bmatrix} 27 & 64,17809 & 64,50334 & 72,05731 \\ 64,17809 & 161,4961 & 153,3223 & 171,2778 \\ 64,50334 & 153,3223 & 159,6547 & 172,1458 \\ 72,05731 & 171,2778 & 172,1458 & 194,4886 \end{bmatrix}$$

$$[M]^{-1} = \begin{bmatrix} 4,958801 & -0,26567 & -0,43003 & -1,22262 \\ -0,26567 & 0,11177 & 1,04.10^{-15} & 3,95.10^{-15} \\ -0,43003 & 2,22.10^{-16} & 0,180005 & -4.10^{-15} \\ -1,22262 & 3,95.10^{-15} & -3,1.10^{-15} & 0,458117 \end{bmatrix}$$

$$[C] = \begin{bmatrix} 0,37141 \\ 0,19996 \\ -0,1127 \\ 0,1966 \end{bmatrix}$$

Thus:

$$c_0 = 0.37141; c_1 = 0.19996; c_2 = -0.1127; c_3 = 0.1966 \quad (20)$$

If we replace expression (20) into Equation (15) and transform, the mathematical equation that express the dependencies of the workpiece roundness on the three technical parameters ( $S_{nf}, V_w, a_f$ ) in the shoe-type centerless grinding process for internal raceway of ball bearings is defined as follows:

$$O_i = 1.14498 \cdot S_{nf}^{0.19996} \cdot V_w^{-0.1127} \cdot a_f^{0.1966} \quad (21)$$

The regression statistics of the developed mathematical models are shown in Table 5. The values of  $R^2$  (0.8685 for the oval-level model) in Table 6 indicate that the model was well fitted with experimental data. It also implies that the oval level model explains 86.85% of the variability of the oval level. Adjusted  $R^2$  values of the oval level model are also shown in the same table; these were 0.8634 (86.34%), indicating good correlations.

**Table 6.** Regression statistics for regression equations.

Sour	Oval Level Model ( $O_i$ )
$R^2$	0.8685
Adjusted $R^2$	0.8634
Standard Error ( $\theta$ )	4.58
The dispersion ( $\sigma$ )	2.94

The standard error ( $\theta$ ) and the dispersion ( $\sigma$ ) indicate the predictive ability of the model. Based on the prediction values and experimental data values for the above various sets of input data, the program calculates the average value of the standard error  $\theta = 4.58\%$  and the dispersion of the error  $\sigma = 2.94$ . The result of the experiment indicates that the difference between experimental values and mathematical model values is small. Therefore, this calculation method can be completely used to accurately predict the oval level of the part in the shoe-type centerless grinding process for the internal raceway of ball bearings.

Based on the values predicted by Equation (21) according to the input data sets and the application of Matlab software version 2021, the graphs showing the influence of the input variables on the part's oval are determined as shown in the Figures 9 and 10 below:

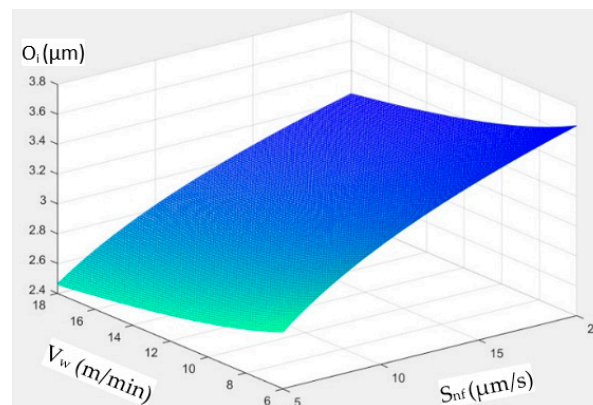


**Figure 9.** The relationship between the oval level of part  $O_i$  and the input variables  $S_{nf}$ ,  $V_w$ .

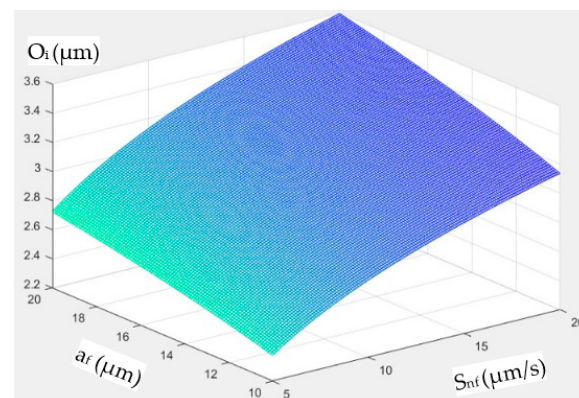


**Figure 10.** The relationship between the oval level of part  $O_i$  and the input variables  $S_{nf}$ ,  $a_f$ .

Based on the above graphs and mathematical functions, it is possible to draw significant conclusions for researching and applying the shoe-type centerless grinding process for the internal raceway of ball bearings as follows:

- When workpiece speed ( $V_w$ ) increased, the oval level ( $O_i$ ) decreased (as shown in Figure 9). In this case, the cause was mainly due to the uneven distribution of metal removal over the whole workpiece circumference. The nature of workpiece rotation is the feed motion per revolution. This motion is created by the combination of the normal feed motion of the workbench and the rotation motion of the workpiece. When increasing the normal feed rate or decreasing the speed of the workpiece, the values of the cutting depth per rotation ( $a_e = S_{nf}/n_w$ ) will increase. Thus, the uneven distribution of the surplus stock over the whole workpiece circumference will increase, leading to an increase in the diameter deviation of the ground part at different cross sections. This leads to an increase in the part's oval level.

- When increasing the value of the normal feed rate ( $S_{nf}$ ), the part's oval level ( $O_i$ ) will increase (as shown in Figures 9 and 10). At the low speed of the workpiece, the influence of the normal feed rate ( $S_{nf}$ ) on the part's oval level ( $O_i$ ) is greater than that at the high speed of the workpiece. When the normal feed rate of fine grinding ( $S_{nf}$ ) increases, the values of cutting depth per rotation will also increase. Thus, the part's oval level ( $O_i$ ) will also increase, and vice versa.
- When the depth of grinding ( $a_f$ ) increases, the part's oval level ( $O_i$ ) will also increase (as shown in Figure 10). When the depth of fine grinding ( $a_f$ ) increases, the amount of removal metal and the uneven distribution of removal metal over the whole workpiece circumference during the grinding process will also increase. Therefore, this leads to an increase in the part's oval level. However, the increase is negligible. This shows that the impact of cutting depth ( $a_f$ ) on the part's oval level ( $O_i$ ) is insignificant.

#### 4. Conclusions

In this study, the effects of the important process parameters on workpiece roundness in the STCG operation for the internal raceway of the 6208 ball bearings were investigated both theoretically and experimentally. Based on that, some conclusions can be drawn as follows:

- The roundness of the bearing raceway in the STCG process depends on the movement trajectory of the workpiece center and the stability of the rotation of the workpiece. The movement trajectory of the workpiece center depends on the mounting angle of the two supports and the deviation from the original shape of the workpiece. It was observed that the value  $b_n^*$  will determine the workpiece roundness. The value of the coefficient  $b_n^*$  depends on the mounting angles of the two shoes ( $\beta, \gamma$ ).
  - + If  $b_n^* = 0$ , the deviation from the original shape of the workpiece will not be corrected.
  - + If  $b_n^* > 0$ , the roundness deviation of the workpiece will be corrected.
  - + If  $b_n^* < 0$ , the original shape deviation of the workpiece during grinding will increase.

Although similar conclusions have been reached by other researchers, the methodology and analysis presented in this study are new.

- In the shoe-type centerless grinding process for the internal raceway of ball bearings, the roundness of the bearing raceway is also affected by the offset between the rotational centers of the workpiece and the magnetic drivehead ( $e$ ), the normal feed rate ( $S_{nf}$ ), the speed of the workpiece ( $n_w$ ), and the grinding depth ( $a_f$ ).
  - + The number of parts in a single cycle ( $N_i$ ) does not affect the part's oval ( $O_i$ ).
  - + When increasing the value of the normal feed rate ( $S_{nf}$ ), the part's oval level ( $O_i$ ) will increase, and vice versa. At the low speed of the workpiece, the influence degree of the normal feed rate ( $S_{nf}$ ) on the part's oval level ( $O_i$ ) is greater than that at the high speed of the workpiece.
  - + When workpiece speed ( $V_w$ ) increased, the oval level ( $O_i$ ) decreased, and vice versa.
  - + When the depth of grinding ( $a_f$ ) increases, the part's oval level ( $O_i$ ) will also increase.
  - + When the offset between the rotational centers of the workpiece and the magnetic drivehead is 0.4 mm, the ovality and 3-sided distortion of the grinding part will be smaller than that when adjusting the eccentricity of 0.3 mm.

Based on the results, a guideline for selecting initial process parameters can be easily formed to ensure the roundness of the bearing raceway in the STCG operation for the internal raceway of 6208 ball bearings on the 3MK136B grinder. However, more research is needed in the near future to improve the performance of the STCG process for the internal raceway of ball bearings.

**Funding:** This research is funded by University of Economics–Technology for Industries (UNETI). I am working at UNETI. This is a public university, training bachelors and engineers in many different majors, directly under the Ministry of Industry and Trade of Vietnam. The UNETI was established in 2007, on the basis of upgrading the College of Industrial Technical Economics I.

**Institutional Review Board Statement:** Not applicable.

**Informed Consent Statement:** Not applicable.

**Data Availability Statement:** The data presented in this study are available on request from the corresponding author. The data are not publicly available due to experimental privacy reasons.

**Conflicts of Interest:** The author declares no conflict of interest.

## Nomenclature

$O_i$ :	The oval of groove bottom diameter ( $\mu\text{m}$ )
$e$ :	The offset between the rotational centers of the workpiece and the magnetic drivehead (mm)
$\beta$ :	Front shoe angle
$\gamma$ :	Rear shoe angle
$S_{nf}$ :	Normal feed rate for fine grinding ( $\mu\text{m}/\text{min}$ )
$V_w$ :	Workpiece speed (m/min).
$V_s$ :	Grinding speed (m/min)
$a_f$ :	The depth of fine grinding ( $\mu\text{m}$ )
$N_p$ :	The number of ground parts (part)
STCG:	Shoe-type centerless grinding

## References

- Pang, G.; Qi, X.; Ma, Q.; Zhao, X.; Wen, C.; Xu, W.; Peng, Y. Surface Roughness and Roundness of Bearing Raceway Machined by Floating Abrasive Polishing and Their Effects on Bearing's Running Noise. *Chin. J. Mech. Eng.* **2014**, *27*, 543–550. [\[CrossRef\]](#)
- Jiang, J.; Ge, P.; Sun, S.; Wang, D. The theoretical and experimental research on the bearing inner ring raceway grinding process aiming to improve surface quality and process efficiency based on the integrated grinding process model. *Int. J. Adv. Manuf. Technol.* **2017**, *93*, 747–765. [\[CrossRef\]](#)
- Chang, Z.; Jia, Q.; Yuan, X.; Chen, Y. Optimization of the grinding process to improve the surface integrity of bearing raceways. *Int. J. Adv. Manuf. Technol.* **2017**, *91*, 4243–4252. [\[CrossRef\]](#)
- Chang, Z.; Jia, Q. Optimization of grinding efficiency considering surface integrity of bearing raceway. *SN Appl. Sci.* **2019**, *1*, 679. [\[CrossRef\]](#)
- Tuan, N.A. Multi-Objective Optimization of Process Parameters to Enhance Efficiency in the Shoe-Type Centerless Grinding Operation for Internal Raceway of Ball Bearings. *Metals* **2021**, *11*, 893. [\[CrossRef\]](#)
- Yan, Z.; Fan, S.; Xu, W.; Zhang, Z.; Pang, G. Profile Evolution and Cross-Process Collaboration Strategy of Bearing Raceway by Centerless Grinding and Electrochemical Mechanical Machining. *Micromachines* **2023**, *14*, 63. [\[CrossRef\]](#) [\[PubMed\]](#)
- Zhou, S.S.; Gartner, J.R.; Howes, T.D. On the Relationship between Setup Parameters and Lobing Behavior in Centerless Grinding. *CIRP Annals* **1996**, *45*, 341–346. [\[CrossRef\]](#)
- Cui, Q.; Ding, H.; Cheng, K. An analytical investigation on the workpiece roundness generation and its perfection strategies in centreless grinding. *J. Eng. Manuf.* **2015**, *229*, 409–420. [\[CrossRef\]](#)
- Rowe, W.B. Rounding and stability in centreless grinding. *Int. J. Mach. Tools Manuf.* **2014**, *82–83*, 1–10. [\[CrossRef\]](#)
- Sakae, Y. Out-of-roundness characteristics of centerless grinding. *Proc. Fujihara Meml. Fac. Eng. Keio Univ.* **1960**, *13*, 17–48.
- Zhou, S.S.; Gartner, J.R.; Howes, T.D. Lobing Behavior in Centerless Grinding—Part I: Stability Estimation. *J. Dyn. Syst. Meas. Control* **1997**, *119*, 153–159. [\[CrossRef\]](#)
- Furukawa, Y.; Miyashita, M.; Shiozaki, S. Vibration analysis and work-rounding mechanism in centerless grinding. *Int. J. Mach. Tool Des. Res.* **1971**, *11*, 145–175. [\[CrossRef\]](#)
- Zhang, B.; Gan, Z.; Yang, Y.; Howes, T.D. Workholding Stability in Shoe Centerless Grinding. *J. Manuf. Sci. Eng.* **1999**, *121*, 41–48. [\[CrossRef\]](#)

14. Zhang, H.; Lieh, J.; Yen, D.; Song, X.; Ru, X. Geometry Analysis and Simulation in Shoe Centerless Grinding. *ASME 2001 Int. Mech. Eng. Congr. Expo.* **2003**, *125*, 304–309. [[CrossRef](#)]
15. Zhang, H.; Lieh, J.; Yen, D. Dynamic performance of shoe centreless grinding. *Proc. Inst. Mech. Eng. Part B J. Eng. Manuf.* **2004**, *218*, 939–947. [[CrossRef](#)]
16. Charmley, J.E. Geometric and dynamic analysis of shoe-type centerless grinding. Ph.D. Thesis, Master of Science in Mechanical Engineering. Massachusetts Institute of Technology, Cambridge, MA, USA, February 1992.

**Disclaimer/Publisher’s Note:** The statements, opinions and data contained in all publications are solely those of the individual author(s) and contributor(s) and not of MDPI and/or the editor(s). MDPI and/or the editor(s) disclaim responsibility for any injury to people or property resulting from any ideas, methods, instructions or products referred to in the content.